

# Integration of Photonic Bandgap Composites with Piezoelectric Actuators for Rejection Wavelength Tuning

Stephen H. Foulger\*, Amanda C. Lattam, Ping Jiang<sup>†</sup> and John Ballato

School of Materials Science and Engineering  
Center for Optical Materials Science and Engineering Technologies  
Clemson University  
Clemson, SC 29634

David E. Dausch, Sonia Grego, and Brian R. Stoner

Microelectronics Center of North Carolina  
3021 Cornwallis Road, P.O. Box 12889  
Research Triangle Park, NC 27709-2889

June 10, 2002

## Abstract

Physically robust photonic bandgap (PBG) composites based on electrostatically stabilized polymeric colloidal particles are presented. The glass transition ( $T_g$ ) of the composites can be varied over a large temperature range through the selection of the monomer(s) used to fabricate the composites. Composites with a subambient  $T_g$  exhibited a mechanochromic response and were integrated with a piezoelectric bimorph actuator to produce a prototype device which exhibited a fully reversible tunable rejection wavelength, capable of a ca.  $\pm 86$  nm (172 nm full range) stop band shift.

## 1 Introduction.

Since the original observation[1, 2] that three dimensional periodic dielectric structures could exhibit a photonic bandgap (PBG), considerable attention has been focused on developing these materials into a form which is suitable for use in photonic applications. Unfortunately, the general exploitation of visible photonic crystals as devices has been hindered by the difficulties in creating physically robust 3D periodic dielectric structures with a feature size comparable to the wavelength of visible light, as well as achieving dielectric contrasts that result in a forbidden gap that overlaps in all directions within the Brillouin zone. Though a number of groups[3-7] have made progress applying conventional microlithographic techniques to this end, this objective remains a challenge employing

---

\*To whom correspondence should be addressed; foulger@clemson.edu.

<sup>†</sup>Department of Chemistry

these techniques. The fabrication of 3D periodic structures by self organization at the tens-to-hundreds of nanometers scale, such as colloidal crystals[8-13], are now receiving growing attention. Systems exhibiting self-assembly characteristics hold promise as a practical route to generating photonic crystals, possibly with a complete bandgap[14].

A crystalline colloidal array (CCA) is a three dimensionally ordered lattice of self-assembled monodisperse colloidal particles, most commonly amorphous silica or a polymer latex, dispersed in aqueous or non-aqueous media[9, 15, 16]. At high particle concentrations, long-range electrostatic interactions between particles result in a significant inter-particle repulsion which yields the adoption of a minimum energy colloidal crystal structure with either BCC or FCC symmetry[10-12]. The ordering of the particles in the media results in spatial periodicities that range from ca.  $10^2$ - $10^3$  nm, resulting in optical bandgap effects.

## 2 Experimental.

**PBG composite synthesis.** Unfortunately, the low elastic modulus ( $10^{-2}$ - $10^{-3}$  Pa)[16-18] exhibited by a liquid dispersion results in weak shear, gravitational, electric field, or thermal forces having the propensity to disturb the crystalline order and is a severe drawback to the practical application of CCAs in photonic devices.

Recently, approaches to develop robust network matrixes have been pioneered to stabilize both organic and inorganic arrays[19, 20] through an *in situ* polymerization of a monomer around the ordered arrays. Asher and co-workers developed the technique of stabilizing all-organic CCAs through the encapsulation in hydrogel networks, referred to as a polymerized crystalline colloidal arrays (PCCA)[21-23]. These PCCA films contain at least 30 vol % of water, resulting in their fragility and propensity for significant changes in optical performance with water content.

Physically robust water-free composites which are based on electrostatically stabilized polymeric colloidal particles have been recently presented[24]. The first phase to fabricating these “PBG composites” requires the stabilization of a CCA through the generation of a hydrogel based PCCA. Although poly(acrylamide) and its derivatives have been established as standard PCCA matrixes[21], our group has focused on the use of poly(ethylene glycol) (PEG) hydrogels to give PEG based PCCAs[23, 25]. Networks based on PEG tend to exhibit a wider range of amphiphilicity and may offer greater compatibility with subsequent chemistry and therefore greater versatility in tuning composite properties.

The CCAs are encapsulated in a hydrogel matrix prepared by an *in situ* photopolymerization procedure. The matrix materials included a monomer of poly(ethylene glycol) methacrylate (PEG-MA,  $M_n = 360$ ), a crosslinker of poly(ethylene glycol) dimethacrylate (PEG-DMA,  $M_n = 550$ ), and a photoinitiator of 2,2-diethoxyacetophenone (DEAP). Once the PCCA is generated, the long range order of the particles and optical characteristics are stable to ionic contamination and minor mechanical deformation, though the mechanical performance of the composite is typical of a “soft” hydrogel with water contents in excess of 80 %.

The next phase in the composite fabrication requires the removal of water through evaporation at ambient conditions and a subsequent vacuum exposure. The dehydrated PCCA film is then swollen in a monomer, for example, 2-methoxyethyl acrylate (MOEA), a monomer which has a strong affinity for the PEG-based matrix of the PCCA. The reswollen PCCA film will again exhibit an angle dependent iridescence. The incorporation of a small quantity of ethylene glycol dimethacrylate and a photoinitiator of 2,2-diethoxyacetophenone (DEAP) into the swollen system, with subsequent photopolymerization, results in a completely water-free composite which exhibits PBG properties and improved mechanical performance relative to the hydrogel PCCA.

**Device fabrication.** A device (cf., Figure 1) was fabricated that integrated a PBG composite with a piezoelectric bimorph actuator to allow for the electromechanical straining of the composite. The composite was attached to a glass substrate and mounted with a bimorph actuator in a PVC frame, while plastic shims were employed to modify the initial stress state of the composite. The dimensions of the actuator was ca. 32 mm x 13 mm x 0.6 mm, with a maximum force output of  $\pm 0.22$  N for a  $\pm 120$  V input, while the PBG composite was ca. 2 mm x 2 mm x 0.5 mm.

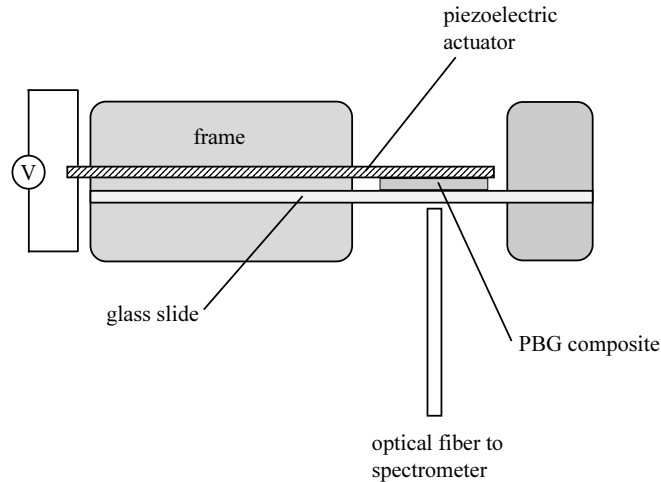


Figure 1: Schematic of stop band tuning device composed of PBG composite with piezoelectric bimorph actuator.

The reflectance spectra of the composites were collected on an Ocean Optics PC2000 fiber optic spectrometer with incident light normal to the plate surface. Spectra were collected between the wavelengths of 300 to 900 nm. This spectrometer was employed for static tuning measurements and had a resolution of ca. 1.5 nm, while a second spectrometer was fabricated which employed a light source with a double monochromator and a photomultiplier tube for radiation detection. This spectrometer was employed for dynamic measurements, allowing for 1 ms time resolution at a fixed wavelength. The refractive index of the composites was measured with a Metricon 2010 wave guide coupler operating at a wavelength of 633 nm. All measurements were performed at ca. 23 °C.

### 3 Results and Discussion.

**PBG composite characterization.** The dynamic mechanical characterization of PBG composites encapsulated in various monomers is presented in Figure 2. A 2-methoxyethyl acrylate based system exhibits a low temperature modulus value of ca.  $5 \times 10^3$  MPa and undergoes a significant drop at an onset temperature of -35 °C. At temperatures greater than this transition point, the modulus is significantly reduced relative to the value in the glassy state, exhibiting a value of ca. 0.7 MPa

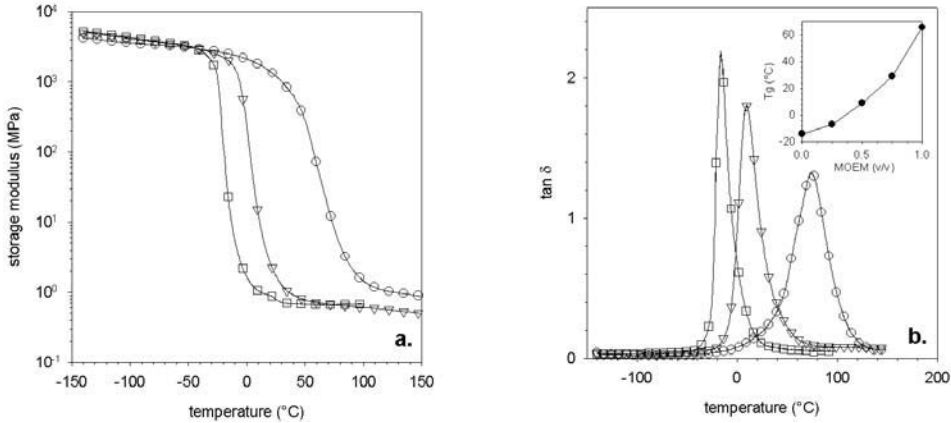


Figure 2: Dynamical mechanical (a.) storage modulus ( $E'$ ) and (b.) loss tangent ( $\tan \delta$ ) of PBG composites encapsulated in 2-methoxyethyl acrylate ( $\square$ ), 2-methoxyethyl methacrylate ( $\circ$ ), and 50/50 2-methoxyethyl acrylate-*co*-2-methoxyethyl methacrylate copolymer ( $\nabla$ ); data acquired at an oscillation frequency of 1 Hz. Inset presents the variation of the observed glass transition in MOEA-*co*-MOEM copolymers with MOEM content.

which is characteristic of the rubbery state. The relaxation exhibited in the dynamic mechanical response of the composite is confirmed by differential scanning calorimetry (DSC), where a maximum change in the heat flow is observed at a temperature of  $-39^\circ\text{C}$ . Beyond the rubbery plateau, the modulus is relatively constant up to a temperature of  $150^\circ\text{C}$ , indicative of the crosslinked nature of the matrix.

The PBG composite is composed of a majority of polymerized 2-methoxyethyl acrylate (e.g.,  $\geq 80$  wt. %), therefore, the transition temperature of the composite most resembles the “pure” PMOEA, where the glass transition ( $T_g$ ) of an uncrosslinked PMOEA has been previously reported in the range of  $-50^\circ\text{C}$  to  $-33^\circ\text{C}$ [26]. The  $T_g$  of the PBG composite can be altered by copolymerization of additional acrylate monomers with MOEA, or through a complete substitution. For instance, substitution of MOEA with 2-methoxyethyl methacrylate (MOEM) results in a hard and glassy PBG composite at  $23^\circ\text{C}$ , with the glass transition occurring at ca.  $40$ - $50^\circ\text{C}$ , while a 50/50 2-methoxyethyl acrylate-*co*-2-methoxyethyl methacrylate copolymer exhibits a glass transition intermediate between the homopolymers, a feature which is confirmed in the corresponding dynamical mechanical loss characteristics of the PBG composites (cf., Figure 2).

The ability to tune the  $T_g$  of a PBG composite through a judicious choice in the encapsulation monomer(s) allows for a wide range of coupled optical and mechanical properties. For example, subambient transitions which result in an elastomeric mechanical response of the PBG composite at room temperature allow for the variation of the stop band with stress (i.e., mechanochromic response).

**Mechanochromic response.** It has been previously observed that PBG materials can exhibit a mechanochromic response[19, 22, 25]. This response has been attributed to the affine deformation of the lattice, where a hypsochromic shift of the stopband is in response to a decrease in the interplanar spacing of the particles. In electrostatically stabilized PBG materials, the double layer dictates the lattice parameters these systems can take on. A wide range of interplanar spacings

can be realized even though the actual particle size remains unaltered.

Figure 3 presents a transmission electron micrograph of a PBG composite. The order of the particles and the large interparticle distance, resulting from their electrostatic stabilization prior to encapsulation, is evident. When colloidal crystals composed of a latex are placed in a cell, the crys-

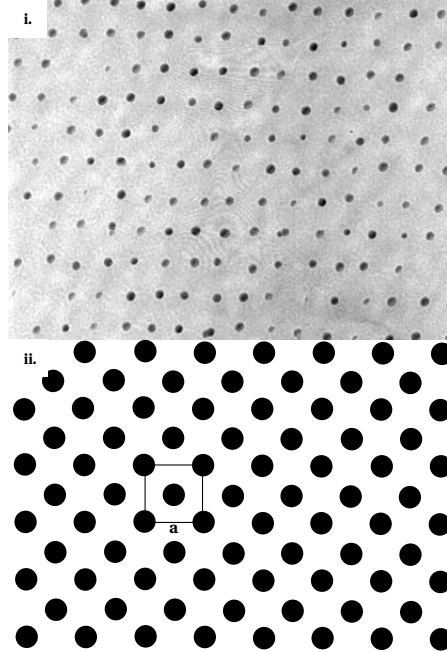


Figure 3: (i.) TEM micrograph of photonic bandgap composite (17K magnification) and (ii.) corresponding schematic of the [100] planes in a FCC crystal.

tals orient with their most densely packed planes parallel to the walls of the container. In the case of CCAs in which the lattice adopts a FCC symmetry, the [111] planes are parallel to the walls[11, 12]. The diffraction characteristics of these systems are most accurately predicted through the application of dynamic diffraction theory, though the Bragg diffraction equation ( $\lambda_o/2 = n_c d_{hkl} \sin \theta$ , where  $\lambda_o$  is the wavelength of the diffracted light in air,  $d_{hkl}$  is the interplanar spacing,  $n_c$  is the refractive index of the composite, and  $\theta$  is the Bragg angle) is a reasonable approximation[27]. In the experimental configuration, unpolarized light is propagated along the [111] direction of the FCC lattice[28]. The observed stop band is then related to the lattice parameter of the conventional cubic unit cell through the Bragg equation and  $a = \sqrt{3}d_{111}$ , while the nearest neighbor distance (i.e., the primitive lattice parameter and spacing between particles at fractional coordinates 0,0,0 and 1/2,0,1/2 of the cubic unit cell) is  $a_p = a/\sqrt{2}$ . The 605 nm stop band observed in the reflectance spectrum of the composite employed in Figure 3 translates into a  $d_{111}$  spacing of 203 nm ( $n_c = 1.489$ ), while  $a$  is 352 nm. The nearest neighbor distance of the polystyrene particles is 249 nm, over twice their 109 nm diameter. In addition, directly measuring the lattice parameter of the

conventional cubic unit cell (a) from Figure 3 results in a value of  $348 \pm 70$  nm, in agreement with the reflectance spectra.

Figure 4 presents the reflection characteristics at normal incidence of a PMOEA-based PBG composite in the stress-free state and under a compressive loading. In the initial stress-free state, the position of the stop band is at 610 nm. Upon applying a 145 kPa compressive stress, the stop band shifts down to a wavelength of 517 nm, a 93 nm variation. Additional compressive stress

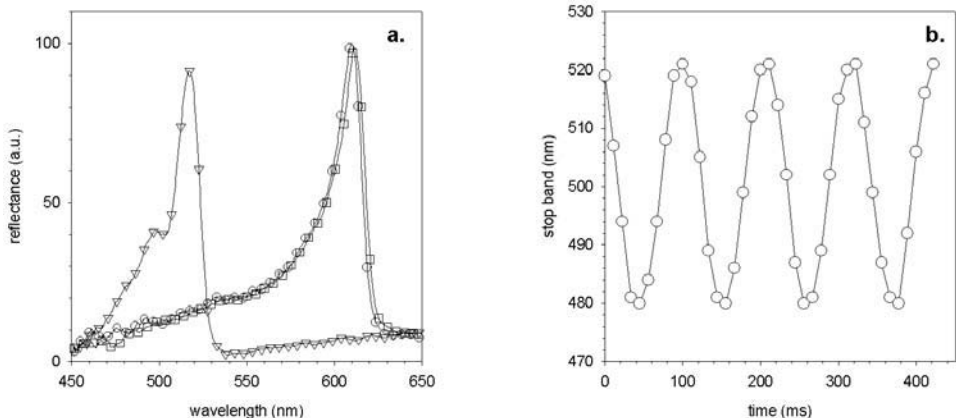


Figure 4: (a.) Reflectance spectra of PMOEA-based PBG composite at normal incidence: original stress-free state ( $\square$ ), under a 145 kPa compressive stress ( $\nabla$ ), and unloaded stress-free state ( $\circ$ ). Intensity of curves have been scaled relative to the original stress-free state. (b.) Variation in observed stopband with cyclic 9% tensile strain of a PMOEA-based PBG composite.

resulted in increasing larger stop band shifts, with shifts of 120 nm being attainable. Assuming that the stop band can be attributed to the  $d_{111}$  interplanar spacings, the strain ( $\epsilon = (\lambda - \lambda_0)/\lambda_0$ ) associated with the 145 kPa stress is -15.2 %. At 23 °C, the PMOEA-based PBG composites are at a temperature above their  $T_g$ . Assuming that their mechanical response can be modeled as rubber-like, a composite with a shear modulus of 310 kPa (cf., Figure 2) would strain ca. -13.5 % under a 145 kPa compressive stress, in agreement with the reflectance results. In addition, the removal of the compressive stress results in the immediate return of the stop band position to the original stress-free state (cf., Figure 4).

Preliminary results indicate that no hysteresis in the optical characteristics are introduced with repeated deformations, as long as the strain level does not result in mechanical degradation of the PBG composite. Figure 4 presents the stop band variation of a film that has been uniaxially strained at 9 % at a frequency of 10 Hz. The wide stop band tuning range and immediate recovery with the cessation of stress suggests that these composites may find utility in optical components. To our knowledge, these environmentally stable (i.e. water free), mechanically robust composites that can exhibit 100 nm or greater band shifts with short recovery times are the first examples of practical tunable photonic crystals with commercial potential. To assess their potential in these applications, a prototype PBG composite/piezoelectric device was fabricated.

**Device characterization.** Static tuning of a device (cf., Figure 1) was conducted with a PMOEA-based PBG composite in both an initial stress-free state and with sufficient tensile pre-stress to strain the composite 12%. Applying a bias to the piezoelectric actuator placed the composite in a

state of stress, where a positive applied voltage resulted in the compression of the PBG composite and a negative voltage placed the composite in tension. Figure 5 presents the change in the position of the observed stop band with actuator bias. Straining the composite in tension resulted in an expansion of the interplanar distance, resulting in a bathochromic shift of the observed stop band, while a compressive strain resulted in a hypsochromic shift. While both the initial stress-free

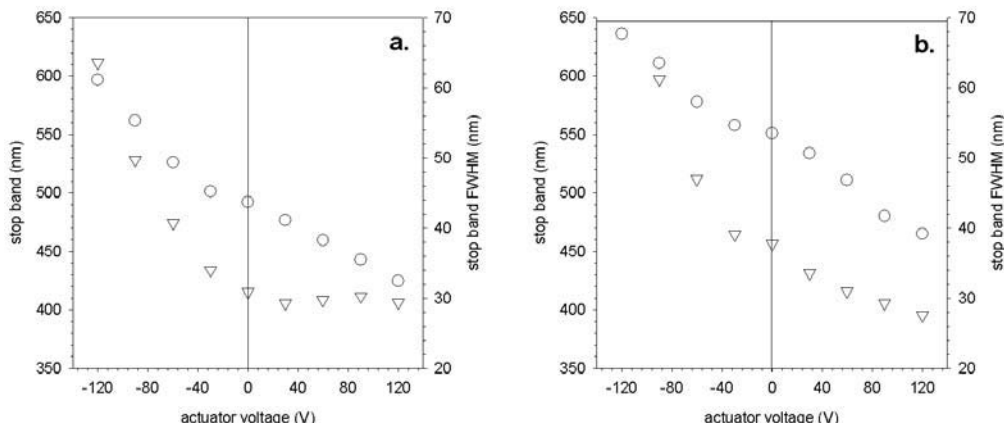


Figure 5: Observed stop band ( $\circ$ ) and peak FWHM ( $\nabla$ ) at various applied voltages to the piezoelectric actuator. A positive applied voltage resulted in the compression of the PBG composite, while a negative voltage put the composite in tension. The PBG composite was mounted in both (a.) an initial stress-free state and with (b.) a tensile pre-strain of ca. 12 % before electromechanical tuning.

and pre-strained device configurations exhibited a similar 171 - 172 nm total tuning range for an applied 240 volt span, the shift in the stop band with bias of the initial stress free device exhibited an inflection at ca. -40 volts (cf., Figure 5). For this device, at the extreme ends of the applied voltage range the ratio of stop band shift to bias was 0.87 nm/V and -0.56 nm/V, respectively, while the pre-strained composite response was relatively linear, exhibiting  $\pm 0.71$  nm/V ratio at a  $\pm 120$  volt bias. In addition, both systems exhibited significant peak broadening with increasing tensile deformation, with a ca. 30 nm FWHM at a +120 volt bias increasing to a ca. 70 nm FWHM at a -120 volt bias. The peaks became broader and less well defined due to the introduction of disorder in the spatial periodicity of the array with the deformation of the composites.

The dynamic tuning characteristics of the coupled composite & actuator device was investigated by utilizing a PBG composite which exhibited a stop band at 508 nm under stress-free conditions.

The composite was then strained at a +60 volt bias and allowed to come to equilibrium, resulting in a shifted stop band at 466 nm. This procedure was then repeated for a -60 volt bias, resulting in a shift of the stop band to 550 nm. The actuator was then driven under a square wave oscillation, employing a  $\pm 60$  volt peak-to-peak amplitude and at frequencies between 1 and 200 Hz. Figure 6 presents the resulting peak intensities at a wavelength of 466 nm, normalized by the intensity at equilibrium. With increasing frequency, the normalized peak intensity is reduced, with observed intensity being less than 10% of the static value at frequencies greater than 200 Hz. At the higher frequencies, the viscoelastic response of the encapsulating PMOEA results in an increase in the storage modulus of the system and a reduced strain in the PBG composite. This response is clearly identifiable in Figure 7 where the intensity of the stop band at 560 nm and corresponding actuator

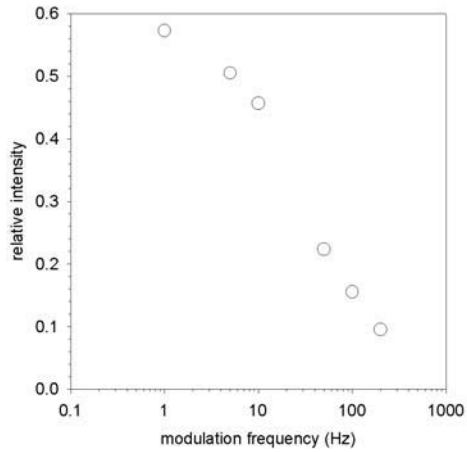


Figure 6: Relative intensity of stop band at 466 nm with increasing frequency of square wave oscillation and  $\pm 60$  volt bias to piezoelectric actuator. Peak normalized relative to the intensity of the stop band at a static bias of +60 volts; see text for details.

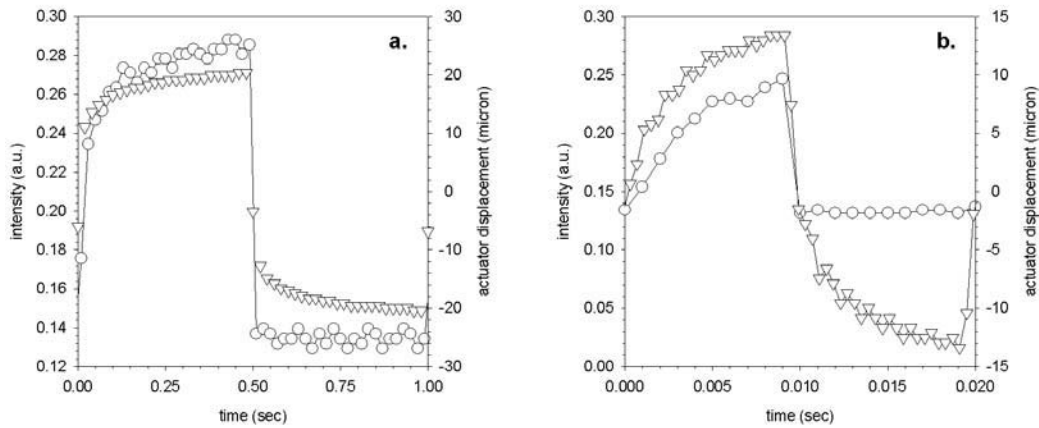


Figure 7: Intensity of reflection peak at 560 nm ( $\circ$ ) and actuator displacement ( $\nabla$ ) with  $\pm 60$  volt bias under a square wave oscillation frequency of (a.) 1 Hz and (b.) 50 Hz.

displacement is presented for a  $\pm 60$  volt bias under a square wave oscillation at frequencies of 1 Hz and 50 Hz. The actuator displacement is reduced due to the higher modulus of the composite at a frequency of 50 Hz relative to 1 Hz. The displacement characteristics of the piezoelectric actuator was a relatively sharp square wave, following the driving waveform closely, when no composite was attached to it. When the composite was attached to the actuator, the viscoelastic nature of the polymeric system appeared to alter the displacement characteristics of the actuator by reducing the rate in which the actuator achieved its maximum displacement. This can be seen in Figure 7 as a curvature in the edge of the square wave, a feature which becomes significantly more pronounced at the higher frequency.

## 4 Conclusion.

Physically robust photonic bandgap (PBG) composites based on electrostatically stabilized polymeric colloidal particles are presented. The glass transition ( $T_g$ ) of the composites can be varied over a large temperature range through the selection of the monomer(s) used to fabricate the composites. Composites with a subambient  $T_g$  exhibited a mechanochromic response and were integrated with a piezoelectric bimorph actuator to produce a prototype device which exhibited a tunable rejection wavelength. This device was capable of a ca. 172 nm stop band shift with a 240 volt bias. The wide range of coupled optical and mechanical properties of the PBG composites add versatility to potential commercial applications such as tunable filter & lasers, beam steering, and optical switching & modulation.

## 5 Acknowledgements.

The authors would like to thank DARPA (Grant Number: N66001-01-1-8938) for financial support, as well the 3M Corporation through a Non-Tenured Faculty Award (SF, JB)

## References

- [1] E. Yablonovitch. *Phys. Rev. Lett.*, 58:2059, 1987.
- [2] S. John. *Phys. Rev. Lett.*, 58:2486, 1987.
- [3] S. Fan, P. R. Villeneuve, R. D. Meade, and J. D. Joannopoulos. *Appl. Phys. Lett.*, 65:1466, 1994.
- [4] C. C. Cheng and A. Scherer. *J. Vac. Sci. Technol. B*, 13:2696, 1995.
- [5] S. Noda, N. Yamamoto, and A. Sasaki. *Jpn. J. Appl. Phys.*, 35:L909, 1996.
- [6] J. S. Foresi, P. R. Villeneuve, J. Ferrera, E. R. Thoen, G. Steinmeyer, S. Fan, J. D. Joannopoulos, L. C. Kimmerling, H. I. Smith, and E. P. Ippen. *Nature*, 390:143, 1997.
- [7] A. Rosenberg, R. J. Tonucci, and E. A. Bolden. *Appl. Phys. Lett.*, 69:2638, 1996.
- [8] A. M. Walsh and R. D. Coalson. *J. Phys. Chem*, 100:1559, 1994.
- [9] P. A. Hiltner and I. M. Krieger. *J. Phys. Chem.*, 73:2386, 1969.
- [10] N. A. Clark, A. J. Hurd, and B. J. Ackerson. *Nature*, 281:57, 1979.
- [11] Y. Monovoukas and A. P. Gast. 128:533, 1989.
- [12] Y. Monovoukas and A. P. Gast. *Phase Transitions*, 21:183, 1990.
- [13] I. M. Krieger and F. M. O'Neil. *JACS*, 90:3114, 1968.
- [14] K. Busch and S. John. *Phys. Rev. E*, 58:3896, 1998.
- [15] P. A. Hiltner, Y. S. Papir, and I. M. Krieger. *J. Phys. Chem.*, 75:1881, 1971.
- [16] T. Okubo. *Prog. Polym. Sci.*, 18:481, 1993.
- [17] R. J. Carlson and S. A. Asher. *Applied Spectroscopy*, 38:297, 1984.
- [18] T. Okubo. *Colloid Polym. Sci*, 271:873, 1993.
- [19] J. M. Jethmalani and W. T. Ford. *Chem. Mater.*, 8:2138, 1996.
- [20] J. M. Jethmalani, H. B. Sunkara, W. T. Ford, S. L. Willoughby, and B. J. Ackerson. *Langmuir*, 13:2633, 1997.
- [21] S. A. Asher, J. Holtz, J. Weissman, and G. Pan. *MRS Bulletin*, October:44, 1998.
- [22] S. A. Asher, J. Holtz, L. Li, and Z. Wu. *J. Am. Chem. Soc.*, 116:4997, 1994.
- [23] S. H. Foulger, S. Kotha, B. Sweryda-Krawiec, T. Baughman, J. M. Ballato, P. Jiang, and D. W. Smith. *Optics Lett.*, 25:1300, 2000.
- [24] S. H. Foulger, P. Jiang, Y. Ying, A. C. Lattam, D. W. Smith, and J. M. Ballato. *Adv. Mater.*, 13:1898, 2001.

- [25] S. H. Foulger, P. Jiang, A. C. Lattam, D. W. Smith, and J. M. Ballato. *Langmuir*, 17:6023, 2001.
- [26] F. Sun and D. W. Grainger. *J. Polym. Sci. Pol. Chem.*, 31:1729, 1993.
- [27] P. A. Rundquist, P. Photinos, S. Jagannathan, and S. A. Asher. *J. Chem. Phys.*, 91:4932, 1989.
- [28] I. Tarhan and G. H. Watson. *Phys. Rev. Lett*, 763:315, 1996.